[redacted]

Copy 35
RM SL56B13

CASE FILE COPY

NACA

Declassified by authority of NASA
Classification Change Notices No. 209
Dated ** 30 NOV 1970

RESEARCH MEMORANDUM

for the

U. S. Air Force

FREE-FLIGHT TESTS OF 1/10-SCALE REPUBLIC F-105 AIRPLANE WINGS IN THE SUBSONIC TO LOW SUPERSONIC SPEED RANGE TO INVESTIGATE THE POSSIBILITY OF FLUTTER

COORD. NO. AF-224

By Burke R. O'Kelly

Langley Aeronautical Laboratory
Langley Field, Va.

CLASSIFICATION CHANGED
UNCLASSIFIED
TO
By Authority JD30-597 Date 10-19-71

[redacted]

NATIONAL ADVISORY COMMITTEE
FOR AERONAUTICS

WASHINGTON

[redacted]

[redacted]

[redacted]

NATIONAL ADVISORY COMMITTEE FOR AERONAUTICS

RESEARCH MEMORANDUM

for the

U. S. Air Force

FREE-FLIGHT TESTS OF 1/10-SCALE REPUBLIC F-105 AIRPLANE WINGS IN THE SUBSONIC TO LOW SUPERSONIC SPEED RANGE TO INVESTIGATE THE POSSIBILITY OF FLUTTER

COORD. NO. AF-224

By Burke R. O'Kelly

SUMMARY

Three pairs of 1/10-scale Republic F-105 airplane wings have been tested at subsonic to low supersonic speeds in free flight by utilizing rocket-propelled models to investigate the possibility of flutter. The wing plan form was swept back 45° at the quarter-chord line and had an aspect ratio and taper ratio based on the exposed panels of 2.92 and 0.5, respectively. Nominal NACA 65A series airfoil sections in the free-stream direction, 5.5 percent thick near the root and 3.7 percent thick at the tip, were used. The test wings were made so that at 7,000 feet they simulated the full-scale wings at sea level. The wings of the first two tests had 76 percent of the torsional stiffness of the full-scale wings whereas the wings of the third set had 50 percent of the full-scale torsional stiffness.

High-frequency vibrations near a natural wing mode occurred during the test of the first set of wings at maximum speed (Mach number 1.46) and again during the coasting flight (Mach number about 1.08). The second set of wings were tested to a Mach number of 1.43 without either encountering vibrations similar to those experienced in the first test or fluttering. During the test of the third set of wings, a mild flutter of short duration occurred between Mach numbers of 0.94 and 1.04 during the accelerating portion of the flight. No other oscillations were experienced during the remainder of the flight.

[redacted]

INTRODUCTION

At the request of the Air Force, free-flight rocket-propelled model tests at subsonic to low supersonic speeds have been conducted by the Langley Laboratory to investigate the possibility of flutter of 1/10-scale Republic F-105 airplane wings. These wings were supplied by the Air Force and were designed and constructed by Dynamic Devices, Inc. This paper presents the results of tests made on three sets of wings.

The model wings were made so that the mass of the prototype wings in low-level high-speed flight would be simulated by the relatively low-level high-speed flight of the model; that is to say, the mass ratios were nearly equal. The model wings were made less stiff than the scaled stiffness of the prototype so that the model wings at 7,000 feet would be expected to flutter at a Mach number less than the critical flutter Mach number of the full-scale airplane at sea level.

SYMBOLS

b	exponential damping constant, $\frac{1}{t_2 - t_1} \log_e \frac{\text{Amplitude at } t_1}{\text{Amplitude at } t_2}$
c	wing chord of exposed panel normal to quarter-chord line at one-half the length of the leading edge, 0.425 ft
f	frequency, cps
g_t	total-damping coefficient, $\frac{b}{\pi f}$
k	reduced frequency parameter, $\omega c/2V$
M	Mach number
ρ	atmospheric density, slugs/cu ft
t	flight time from launching, sec
V	velocity, fps
ω	frequency, radians/sec

[redacted]

MODELS AND INSTRUMENTATION

Models

The general model arrangement is shown in figure 1, a photograph of one of the models is shown in figure 2(a), and a photograph of a model with its booster in launching position may be seen in figure 2(b).

It may be seen in figure 1 that the main structure of a model consisted of the 5-inch cordite rocket motor. Attached to the forward end of the motor was the telemeter covered by the nose cone. A shrink-fit magnesium tube over the after end of the motor had the wing attachment plates and the vertical fins welded to it.

The wing attachment plates formed a slot which was larger than the root block of the test wings, and when the wings were inserted and fastened by bolts, the remaining space was filled with a thermosetting polyester resin. Past experience has shown that this type of attachment gives a mounting which has more than adequate strength.

Each model was accelerated to a Mach number of about 0.3 by a 3.25-inch booster rocket motor. After separation from the booster, the rocket motor of the model accelerated it through the flutter test range at about 9g. The maximum speed of the test was a Mach number of approximately 1.45. Past experience has shown that longitudinal accelerations on this order have but little effect on flutter buildup.

Weight and balance data for the models are shown in the following table:

	Model 1	Model 2	Model 3
Center of gravity, with fuel, station	47.1	46.7	47.1
Center of gravity, without fuel, station. . .	48.5	47.9	48.3
Weight, with fuel, lb	96.5	98.5	97.2
Weight, without fuel, lb	68.6	70.2	69.0

Test Wings

Three pairs of Republic F-105 flutter wings were tested in this investigation. The wing plan form was swept back 45° at the quarter-chord line and had an aspect ratio and taper ratio based on the exposed panels of 2.92 and 0.5, respectively. Nominal NACA 65A series airfoil sections were used. At a section 5.4 inches outboard of the exposed root, which corresponded to the outer limit of the engine air duct fairing on the full-scale wings, the model airfoil was 5.5 percent thick and at the tip the airfoil was 3.7 percent thick. The geometry of the wings may be seen in figure 1.

Only the stiffness and mass were controlled in the design of these wings. The frequencies obtained, however, were close to those expected. Torsional-frequency agreement was very good and the bending frequencies were low. These low bending frequencies were caused mainly by the tip rib being heavier so that this portion of the wing was stronger and able to withstand aerodynamic and inertia loads.

In order to achieve the nearly equal mass ratios between the scaled wing and the prototype wing, and to obtain the correct torsional stiffness (76 percent of the scaled values for the first two sets of wings and 50 percent for the third set), a light, relatively stiff structure was necessary. A drawing of the wing showing constructional details is shown in figure 3. This figure shows a hollow spar and rib casting as the main structure of the wing. The root attachment, also hollow, was cast integrally with the spar and ribs. Shaped hardwood strips formed the leading and trailing edges. Small lead weights were used where necessary to insure proper mass and inertial characteristics. The gridwork of the spar, the ribs, and the leading and trailing edges was filled with balsa in the manner shown in the typical wing section in figure 3. After the wing was contoured to conform to the desired airfoil shape, a covering of silk was lacquered in place. Provision was made in each wing for the installation of a vibration pickup (fig. 3).

After installation of the wings, the complete model was vibrated in the laboratory using an electrodynamic shaker over which the model was suspended at its center of gravity by a shock cord. The natural frequencies and associated nodal lines determined in this way are shown in figures 4(a), 4(b), and 4(d). The area between the first bending node line and the wing root (fig. 4(a)) felt dead to the fingers and the node line merely bounds the inactive area. The results of the test of model 1 indicated a need of additional wing vibratory information in the high frequency range. Therefore, one of the wing panels to be installed in model 2 was attached to a backstop and was excited directly with the vibrator. The wing was not excited in the low frequency range. The results of the tests made in the high frequency range are shown in figure 4(c). A comparison in the high frequency range shows good agreement at 152 and 158 cycles per second. Agreement at frequencies of 288 and 291 cycles per second is good at the node line nearest the root for the backstop-mounted wing. The node line at 288 cycles per second near the tip was not evident in the model-mounted wing. The 306-cycle-per-second frequency for the model-mounted wing was not evident in the backstop-mounted wing nor was the frequency of 362 cycles per second of the wing on the backstop found in the wing on the model. It is possible that these differences may be due to absence of body modes in the wing mounted alone on the backstop.

[redacted]

Structural influence coefficients were measured in the laboratory on one wing of each pair for models 2 and 3 and are presented in tables I and II. Each wing was mounted to a backstop and the load applied at the locations shown in the tables. A dial gage readable to 10^{-4} inch was placed alternately under each point and read as the load was applied and removed. Only one gage was used since it was found that the addition of the spring constants of multiple gages introduced considerable error. Other wing parameters may be seen in reference 1.

The wing weight was about 4.2 pounds per panel which includes the base block calculated to weigh about 1.8 pounds.

Instrumentation

Each model was equipped with a telemeter which transmitted continuous signals of the quantities to be measured. These quantities, which were the same for all three models, were normal acceleration of each wing provided by vibrometers installed as shown in figure 3, normal acceleration of the model measured near the forward end of the rocket motor, and total pressure.

The vibrometer is a small normal accelerometer which will give a true representation of frequency. Because of its design, however, no reliance can be placed on the values of acceleration derived from it.

Atmospheric conditions prevailing at the times of the model flights were obtained from rawinsonde equipment which provided winds-aloft data as well. The velocity of each model with respect to a ground reference point was determined by a velocimeter radar and the position of each model in space was provided by a pulse-type radar. Motion-picture cameras were used to give photographic records of each flight. Launchings were made at the Langley Pilotless Aircraft Research Station at Wallops Island, Va.

FLIGHT TEST RESULTS

Time histories of the flights showing Mach number, velocity, and atmospheric density are shown in figure 5. Portions of the telemeter records are shown in figure 6.

Model 1

The time history of the flight of model 1 is shown in figure 5(a) and portions of the telemeter record are shown in figures 6(a) and 6(b). These figures show that, as the model reached maximum velocity at a Mach number of 1.46, the wings vibrated briefly at a frequency of 320 cycles per second. As the model coasted from peak velocity, the wings again started to vibrate but at 329 cycles per second. The right-wing vibrations began at a Mach number of 1.11 and, as the frequency increased to 354 cycles per second, the vibrations momentarily damped out at a Mach number of about 1.04. The vibrations begain again (at a Mach number of 1.03) at 420 cycles per second and decreased to about 314 cycles per second as they damped out at a Mach number of 1.01. The left-wing vibrations began at a Mach number of 1.08 at 312 cycles per second and damped out momentarily at a Mach number of 1.05 as the frequency increased to 344 cycles per second. The vibrations began again at a Mach number of 1.03 at 348 cycles per second. As the right wing damped out, the left-wing frequency reduced to 298 cycles per second and remained fairly constant until the oscillations damped out at a Mach number of 0.96. The flight records show that no wing failure occurred. The normal accelerations of the model during the flight did not exceed $\pm 0.3g$.

As a matter of interest, the high amplitude oscillations from the right wing were examined and the total-damping coefficient was obtained from the oscillations by the following relations:

$$g_t = \frac{b}{\pi f}$$

where b is the exponential damping constant and f is the frequency of the oscillation. The resulting variation of damping coefficient with Mach number is plotted in figure 7(a). Although the structural damping was not measured, it was less than 0.03. (See ref. 1.) Shown also in figure 7(a) is the variation of the reduced-frequency parameter k with Mach number during the wing oscillations.

Model 2

A time history of the flight of model 2 is shown in figure 5(b). Although these wings were supposedly the same as those tested on model 1, they did not experience any wing vibrations which could be attributed to flutter, nor did the oscillations as experienced by the first model repeat themselves up to a Mach number of 1.43. However, low-amplitude low-damped oscillations occurred which have been attributed to rough burning of the rocket motor in the model. Normal accelerations experienced by the model during the flight were not greater than 0.8g to -0.1g

Model 3

A time history of the flight of model 3 is shown in figure 5(c) and a portion of the telemeter record is shown in figure 6(c). These figures show that at a Mach number of 0.96 during accelerated flight the wings began to oscillate at 107 cycles per second. These oscillations ended at a Mach number of 1.03 on the left wing as the frequency reached 115 cycles per second, whereas the right-wing oscillation ended at a Mach number of 1.04. No other oscillations were evident up to the maximum speed of the test ($M = 1.47$) nor were the oscillations repeated during the coasting portion of the flight as the altitude increased and dynamic pressure decreased. The normal acceleration of the model during the wing vibrations oscillated at the wing frequency between 0.25g and -0.05g and the maximum normal accelerations during the flight were 0.45g and -0.21g.

As in the case of model 1, the total-damping coefficient g_t was obtained from the right-wing oscillations and the resulting variation of g_t with Mach number is plotted in figure 7(b). Shown also in figure 7(b) is the variation of k with Mach number during the wing oscillation.

CONCLUDING REMARKS

Results obtained from rocket-model flutter tests of three sets of 1/10-scale F-105 airplane wings, one set having less stiffness than the others, do not show the existence of flutter for the full-scale wings in clean condition up to a Mach number of 1.47.

Although one set of wings developed high frequency oscillations near a natural mode of the wing, the full-scale wings should be free of this type oscillation since the higher modes of vibration were not duplicated. Furthermore, a second set of wings (built to be identical to the first set) were free of such vibrations. No flutter was encountered in either of these tests.

A third set of wings, less stiff than the other two sets tested, developed a mild flutter of short duration during accelerated flight. This flutter was not experienced by the wings during the coasting flight as the altitude increased and the dynamic pressure decreased. Since these wings were only half the scaled stiffness in torsion of the full-scale wings, the existence of flutter in the full-scale wings is not indicated.

Langley Aeronautical Laboratory,
National Advisory Committee for Aeronautics,
Langley Field, Va., January 30, 1956.

Burke R. O'Kelly
Burke R. O'Kelly
Aeronautical Research Scientist

Approved: Joseph A. Shortal
Joseph A. Shortal
Chief of Pilotless Aircraft Research Division

JBB

REFERENCE

1. Anon.: Phase II Report P.O. 4-14-23130. Dynamic Devices, Inc., (Dayton, Ohio).

TABLE I.- STRUCTURAL INFLUENCE COEFFICIENTS OF MODEL 2 WING

AT LOAD POINTS INDICATED IN SKETCH

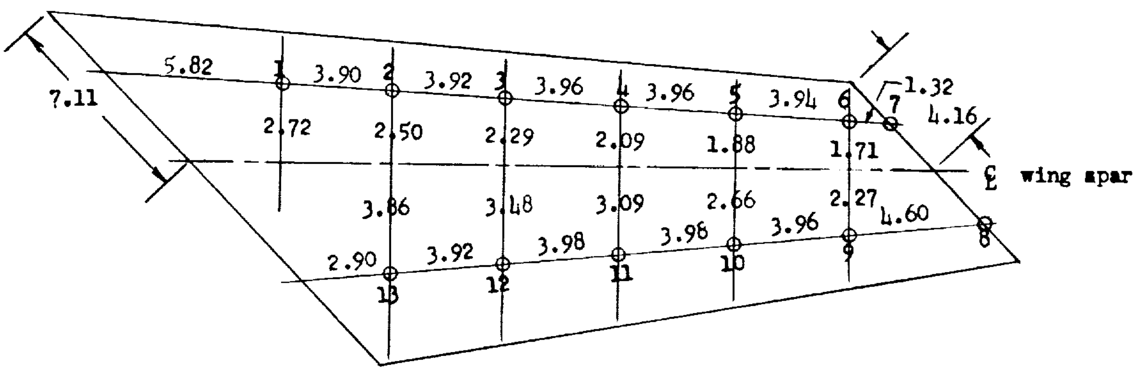

Load points	Deflection in inches × 10^4 at load points, per pound												
	1	2	3	4	5	6	7	8	9	10	11	12	13
1	0	2	2	2	2	4	1	0	2	0	0	0	0
2	0	3	3	3	4	2	3	2	5	0	2	1	0
3	0	2	1	7	8	10	12	12	12	9	6	2	0
4	0	3	8	17	29	39	37	41	34	23	13	5	1
5	0	4	11	26	59	80	90	104	75	46	22	8	2
6	1	5	14	37	87	155	186	212	137	73	31	10	2
7	1	5	15	34	92	179	210	260	154	80	34	12	2
8	0	4	15	38	106	218	263	319	250	119	49	16	3
9	0	4	12	33	76	136	156	228	171	91	39	14	2
10	0	4	10	24	49	76	81	116	95	70	32	11	2
11	0	3	6	13	24	35	34	47	42	33	27	9	2
12	0	3	3	6	10	12	11	13	14	12	10	10	2
13	0	1	2	3	4	3	0	0	1	2	2	2	2

TABLE II.- STRUCTURAL INFLUENCE COEFFICIENTS OF MODEL 3 WING

AT LOAD POINTS INDICATED IN SKETCH

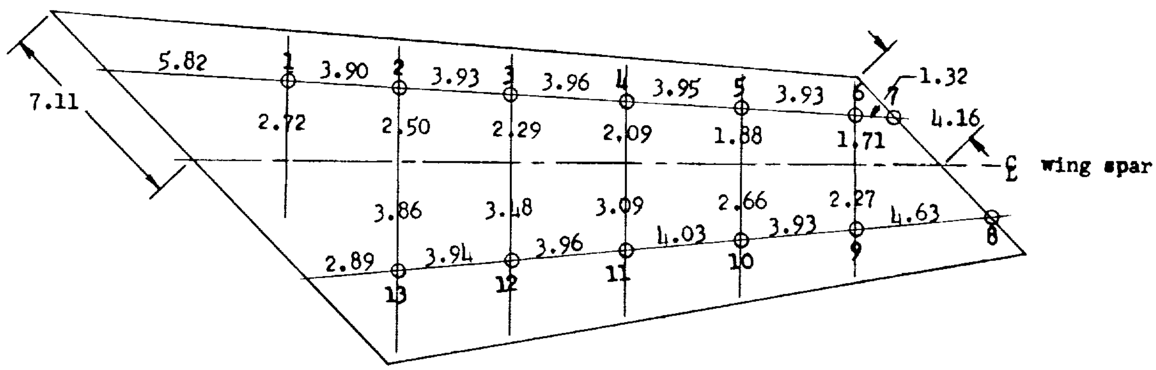

Load points	Deflection in inches × 10^4 at load points, per pound												
	1	2	3	4	5	6	7	8	9	10	11	12	13
1	0	0	0	0	1	0	1	1	1	0	0	0	0
2	0	2	2	3	4	3	5	6	3	3	1	1	0
3	0	2	5	10	14	16	17	17	13	10	5	3	0
4	0	3	10	25	37	48	52	54	39	27	13	5	1
5	0	5	13	37	76	107	120	133	90	57	25	8	2
6	1	6	17	49	110	194	212	244	160	94	38	12	2
7	1	7	18	52	120	211	254	303	181	104	42	13	2
8	0	6	17	55	134	263	301	554	301	154	62	19	3
9	0	4	13	40	92	159	189	293	210	115	49	16	2
10	0	3	9	26	57	90	101	149	115	84	39	13	2
11	0	2	5	13	27	40	45	67	50	41	30	6	2
12	0	1	2	5	9	10	12	18	16	13	10	1	2
13	0	0	0	0	2	2	3	4	3	3	1	2	2

[redacted]

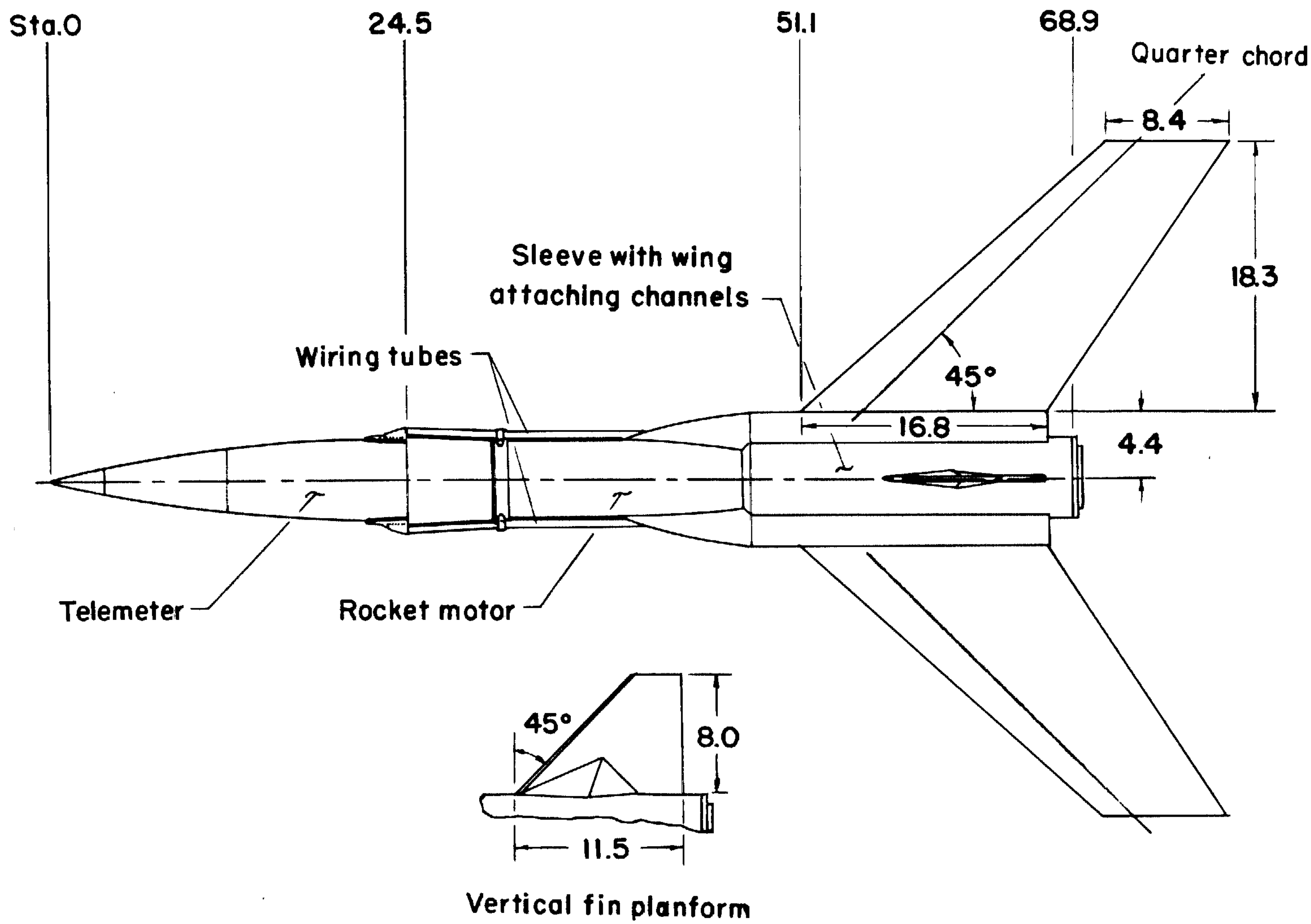

Figure 1.- General arrangement of the model. All dimensions are in inches.

[redacted]

[redacted]

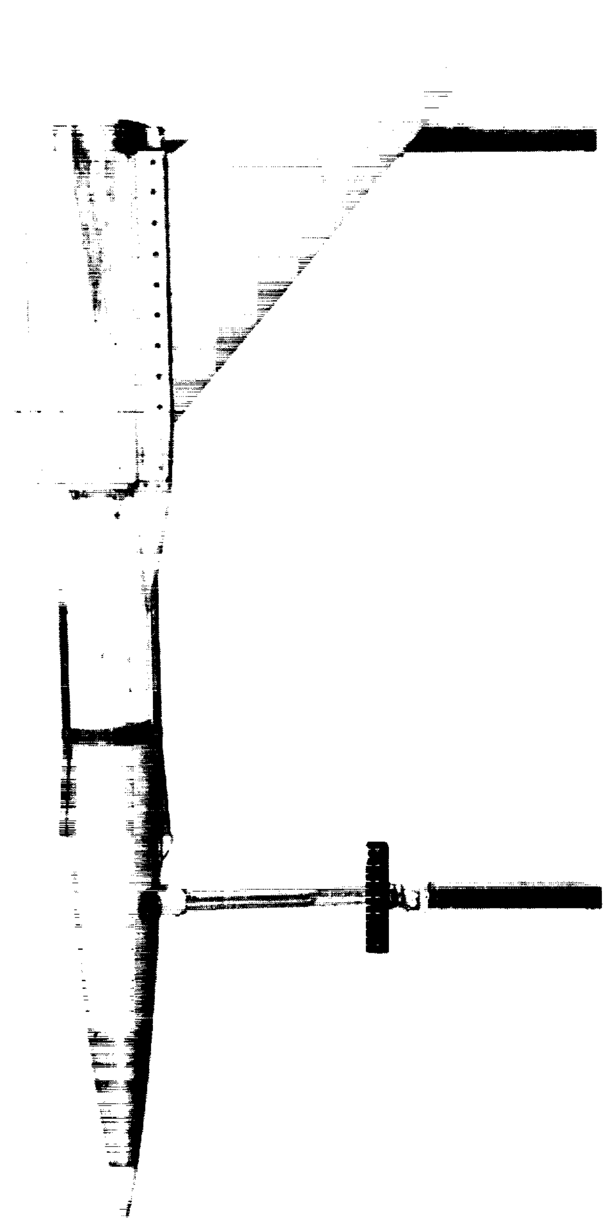

L-86748.1

(a) Model 1.

Figure 2.- Photograph of a model.

[redacted]

 [redacted]

(b) Model 1 and booster. L-87025.1

Figure 2.- Concluded.

[redacted]

[redacted]

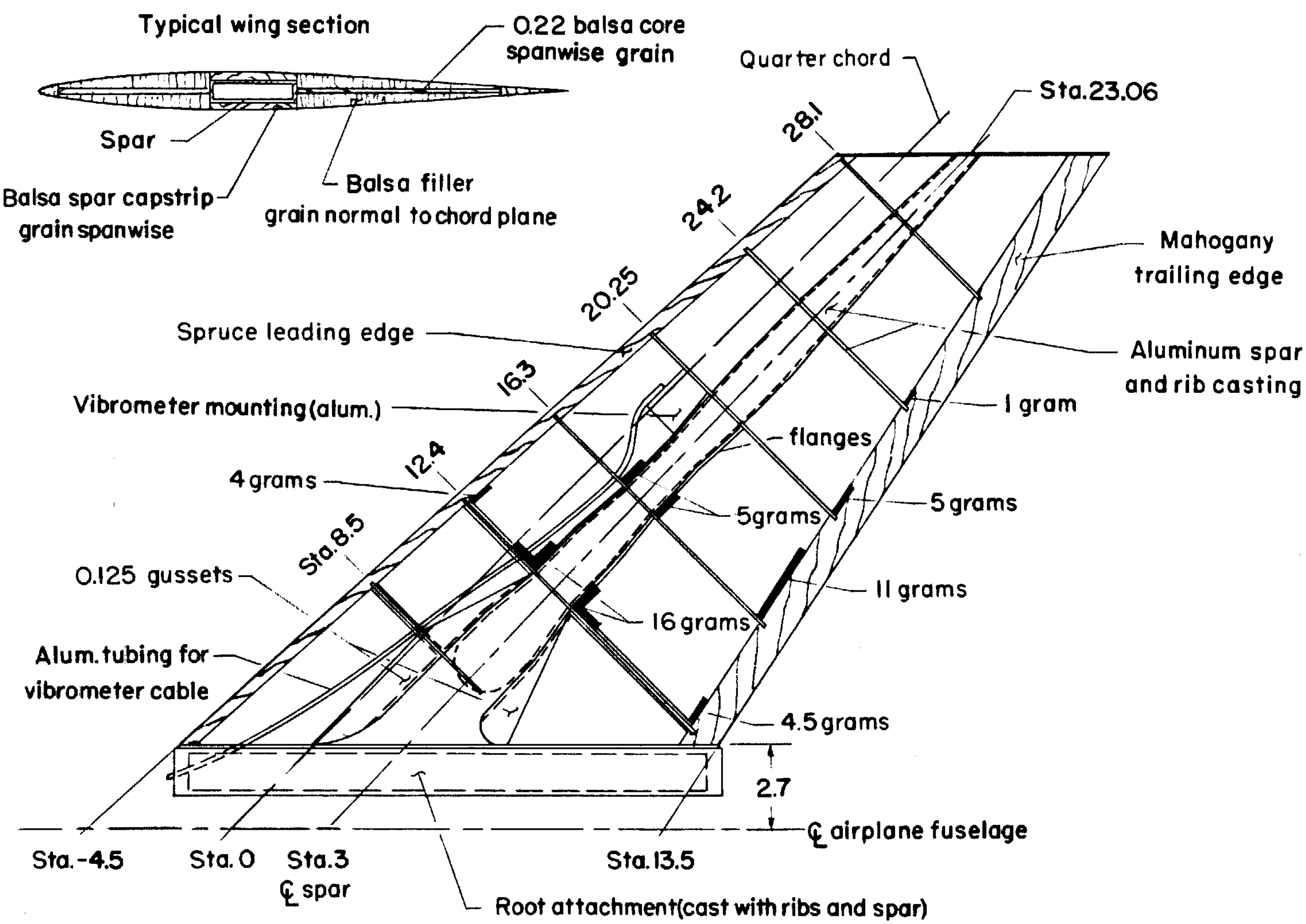

Figure 3.- Constructional details of the wings. All dimensions are in inches.

[redacted]

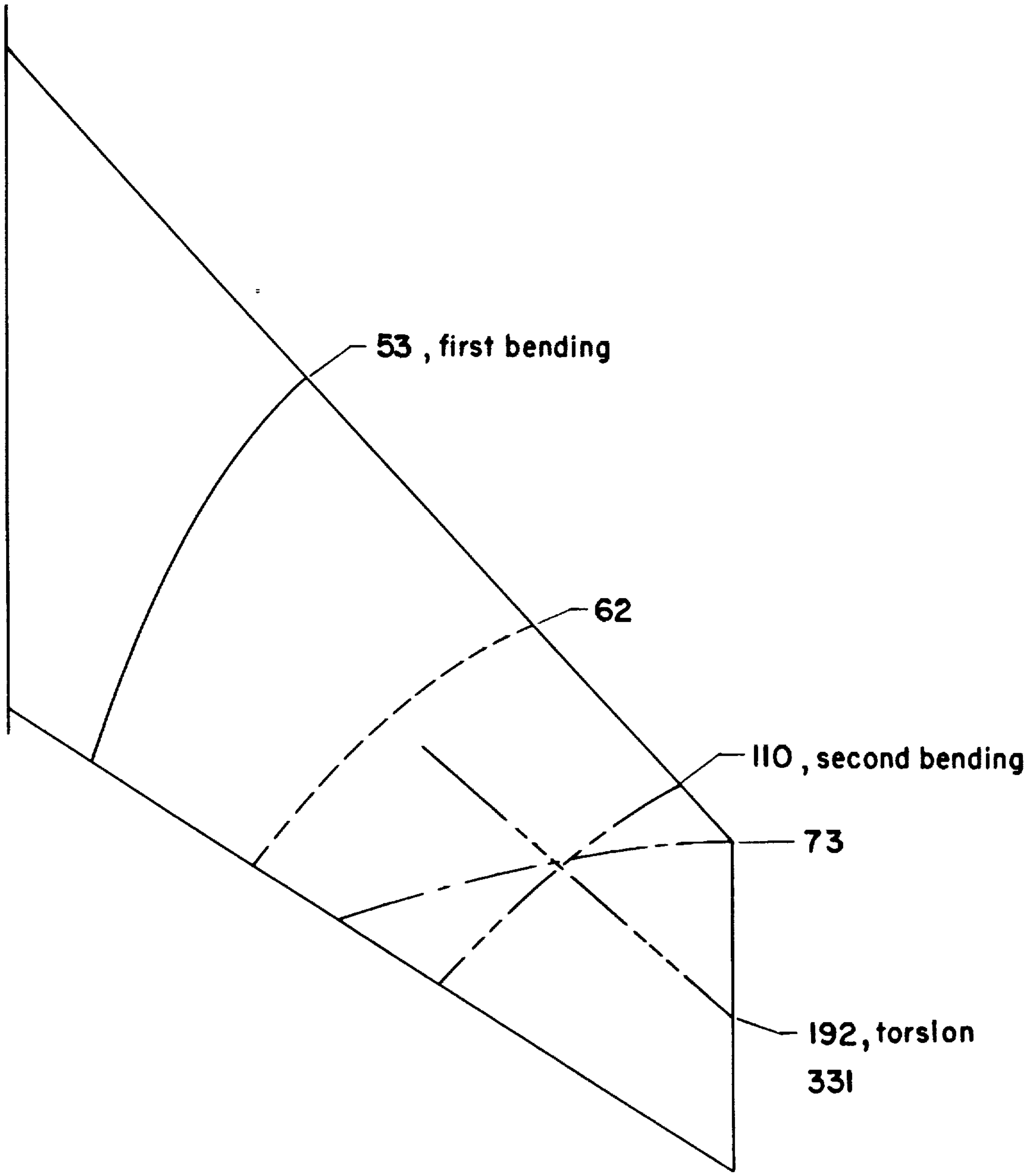

(a) Model 1 wing on model.

Figure 4.- Natural frequencies and node lines of the wings. Wing and node line locations are drawn to scale. Frequencies are in cycles per second.

[redacted]

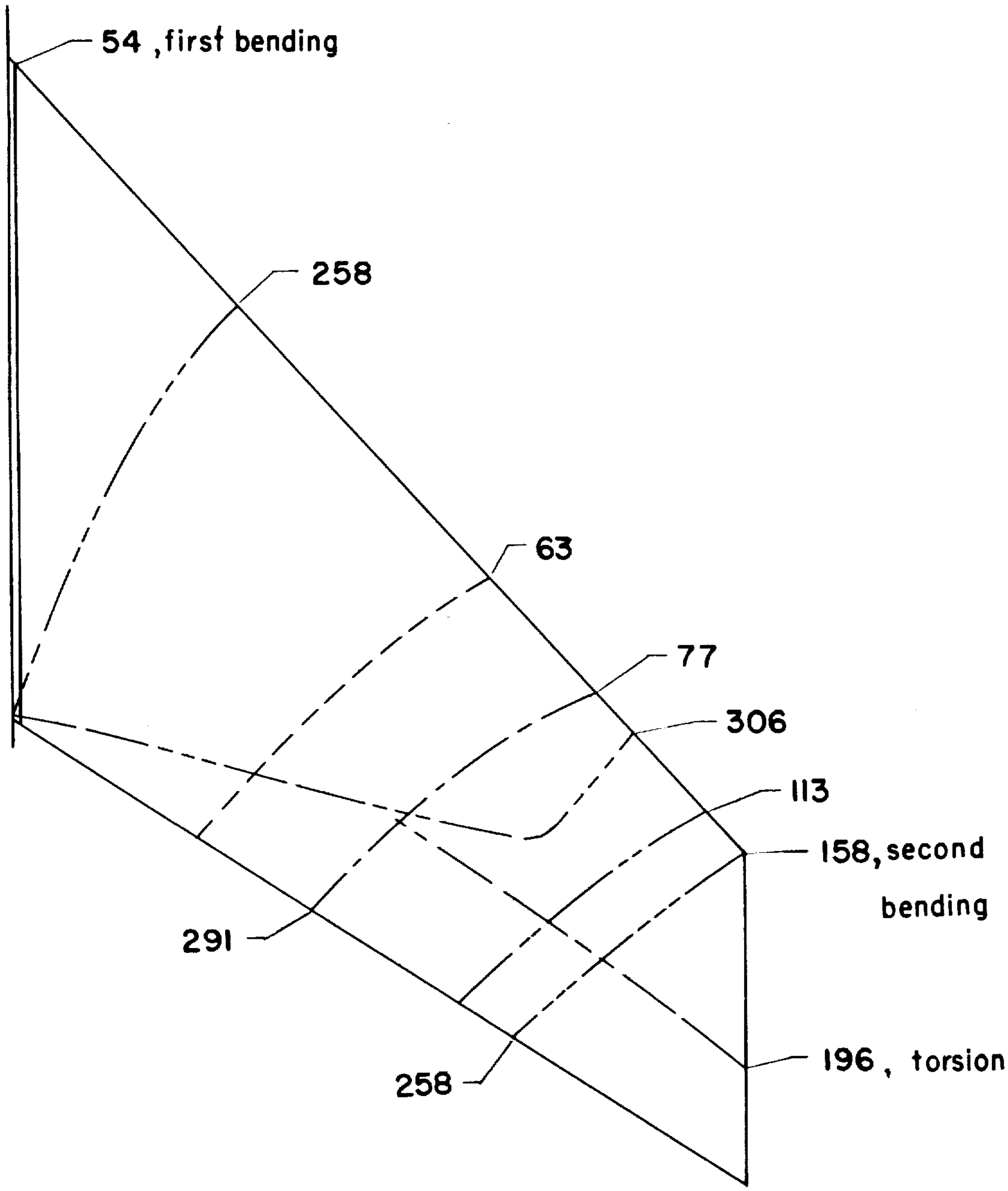

(b) Model 2 wing on model.

Figure 4.- Continued.

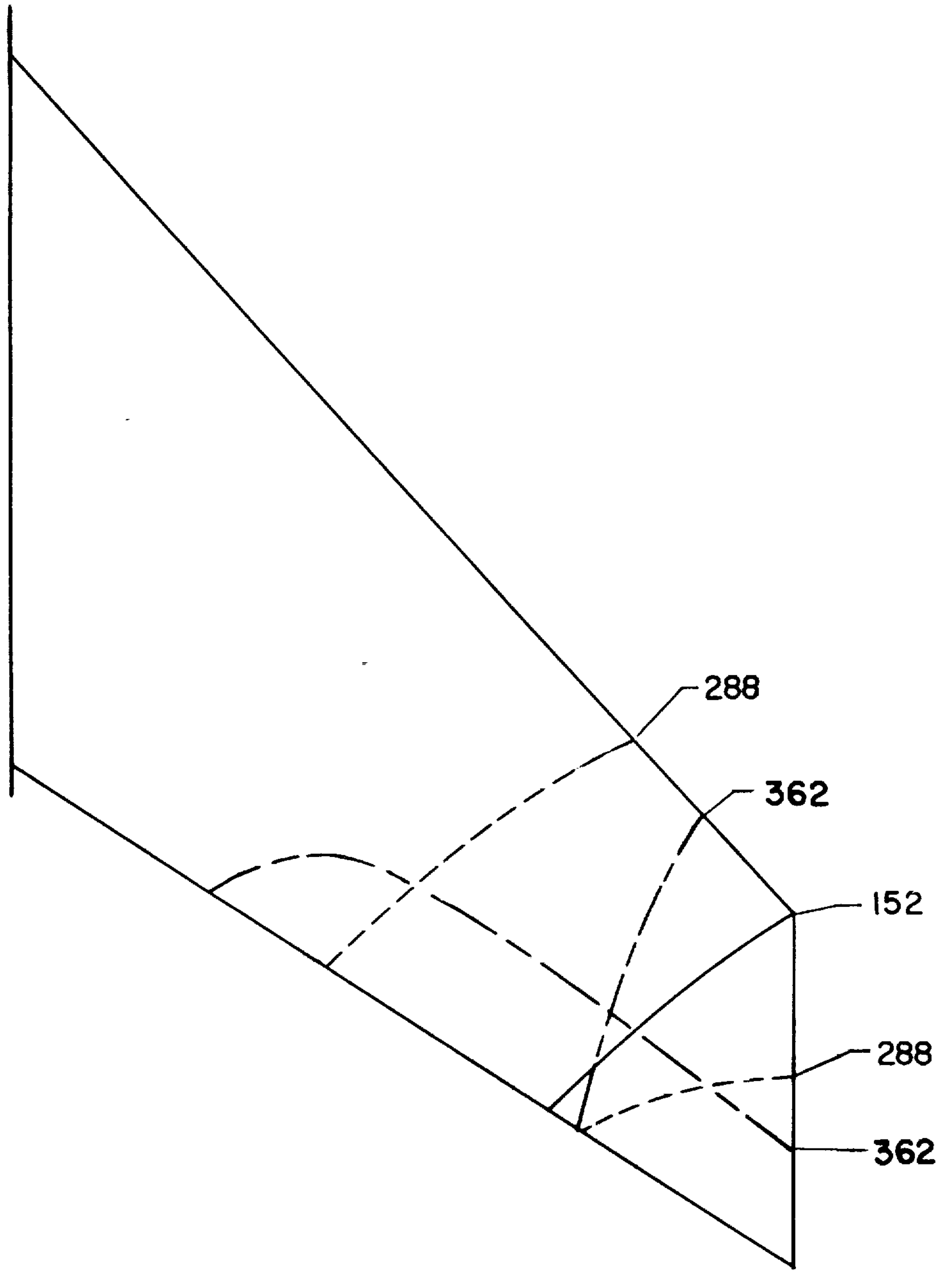

(c) Model 2 wing on backstop.

Figure 4.- Continued.

 [redacted]

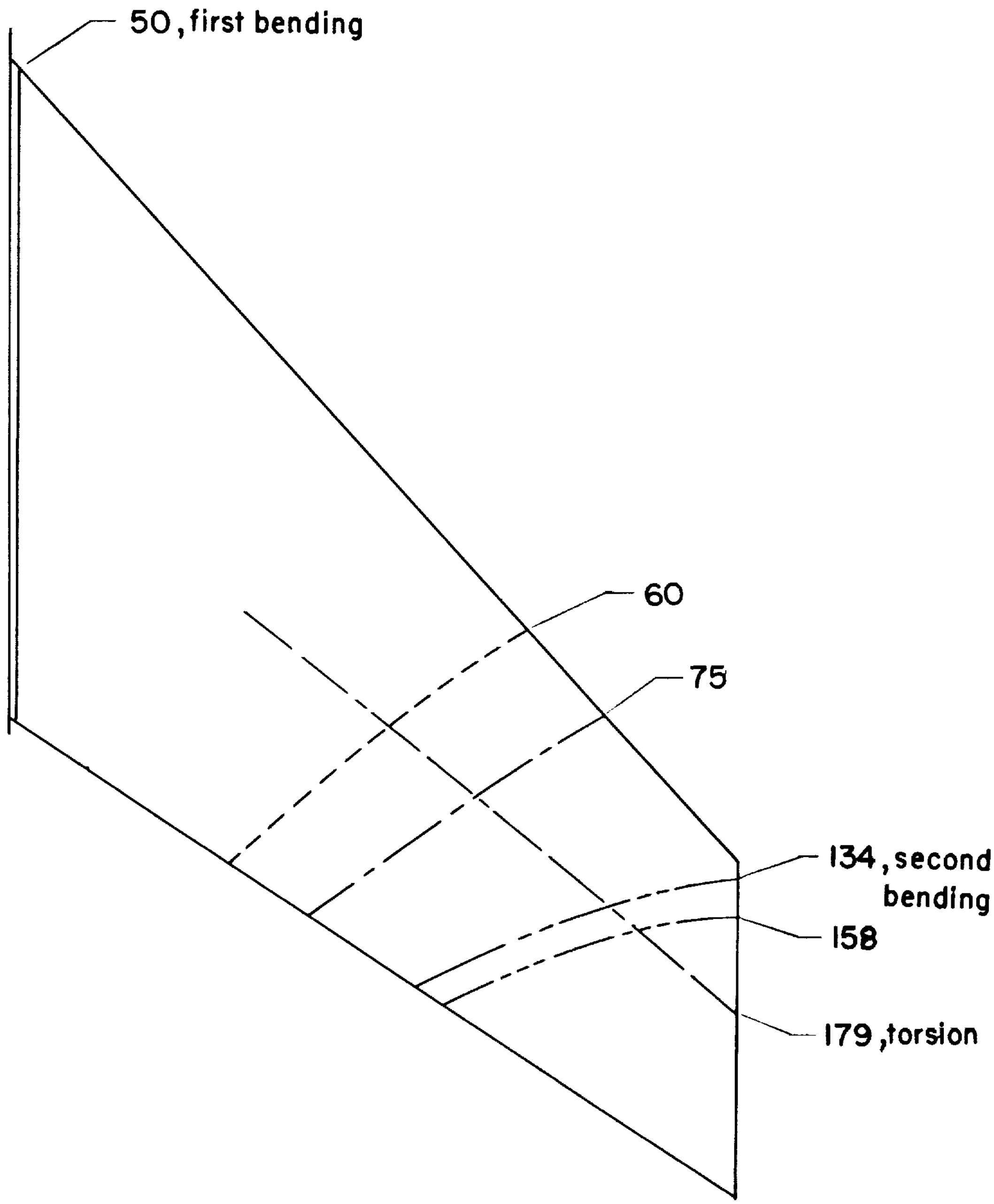

(d) Model 3 wing on model.

Figure 4.- Concluded.

[redacted]

[redacted]

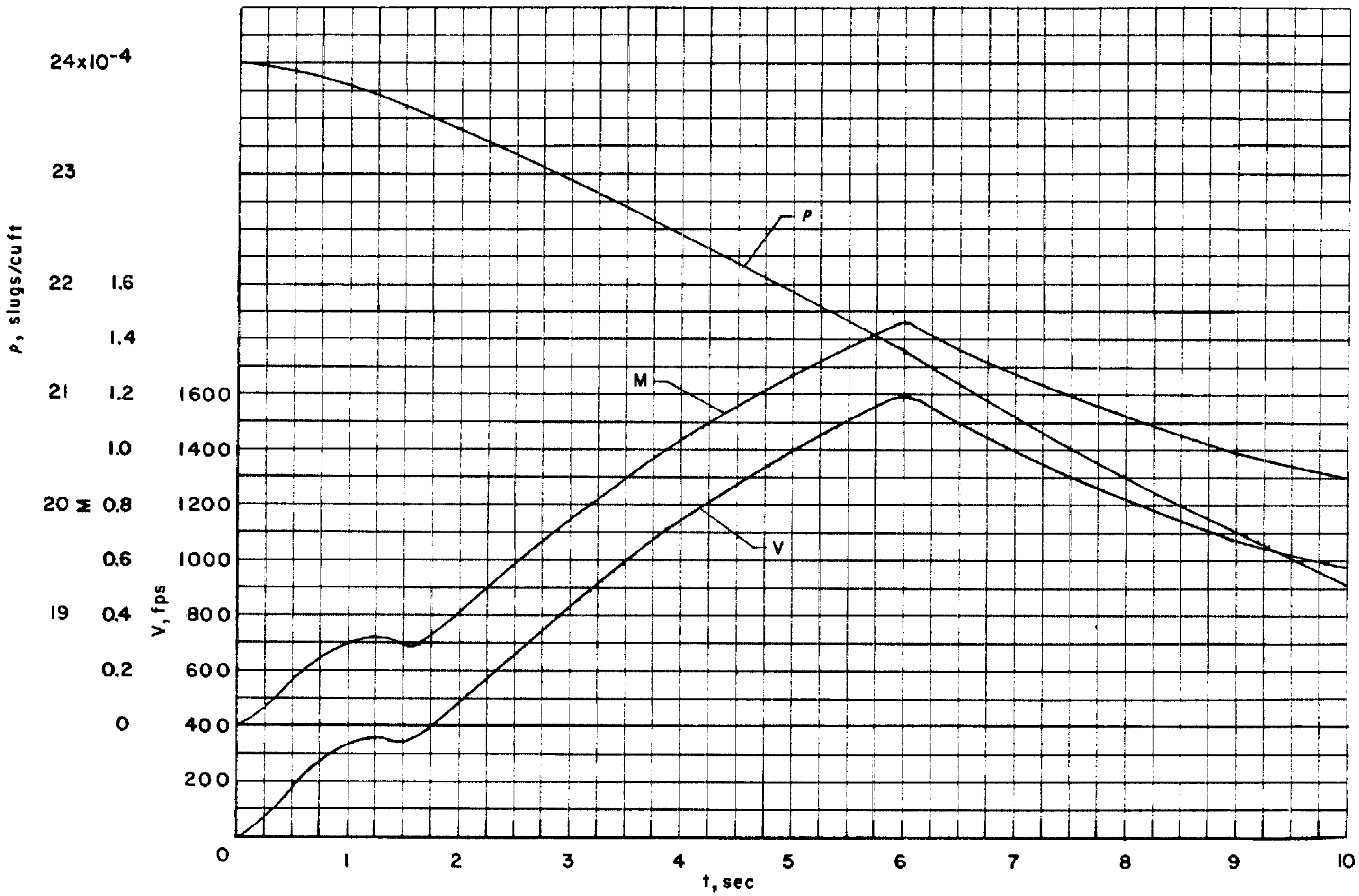

(a) Model 1.

Figure 5.- Time histories showing velocity, Mach number, and air density.

[redacted]

[redacted]

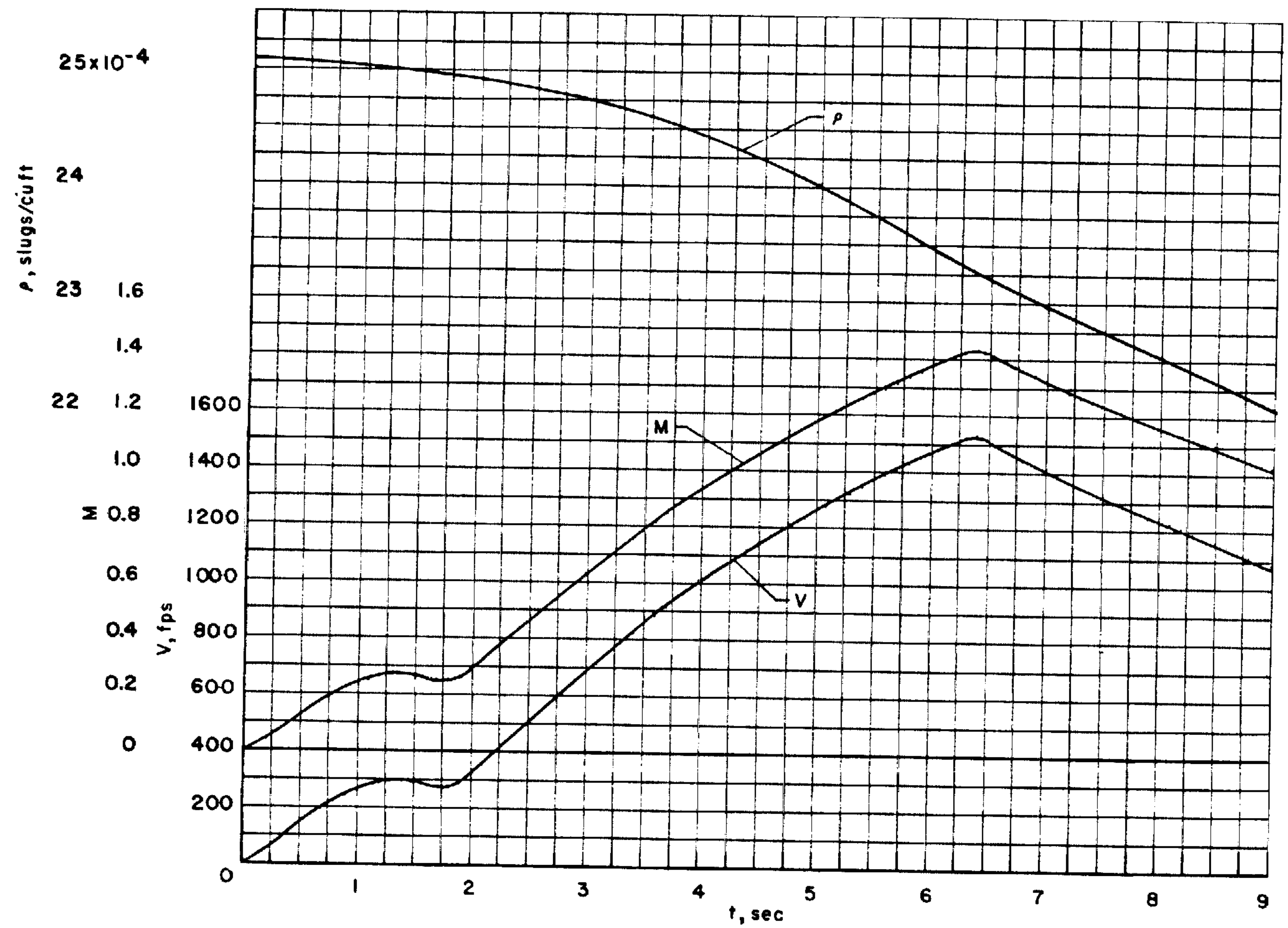

(b) Model 2.

Figure 5.- Continued.

[redacted]

[redacted]

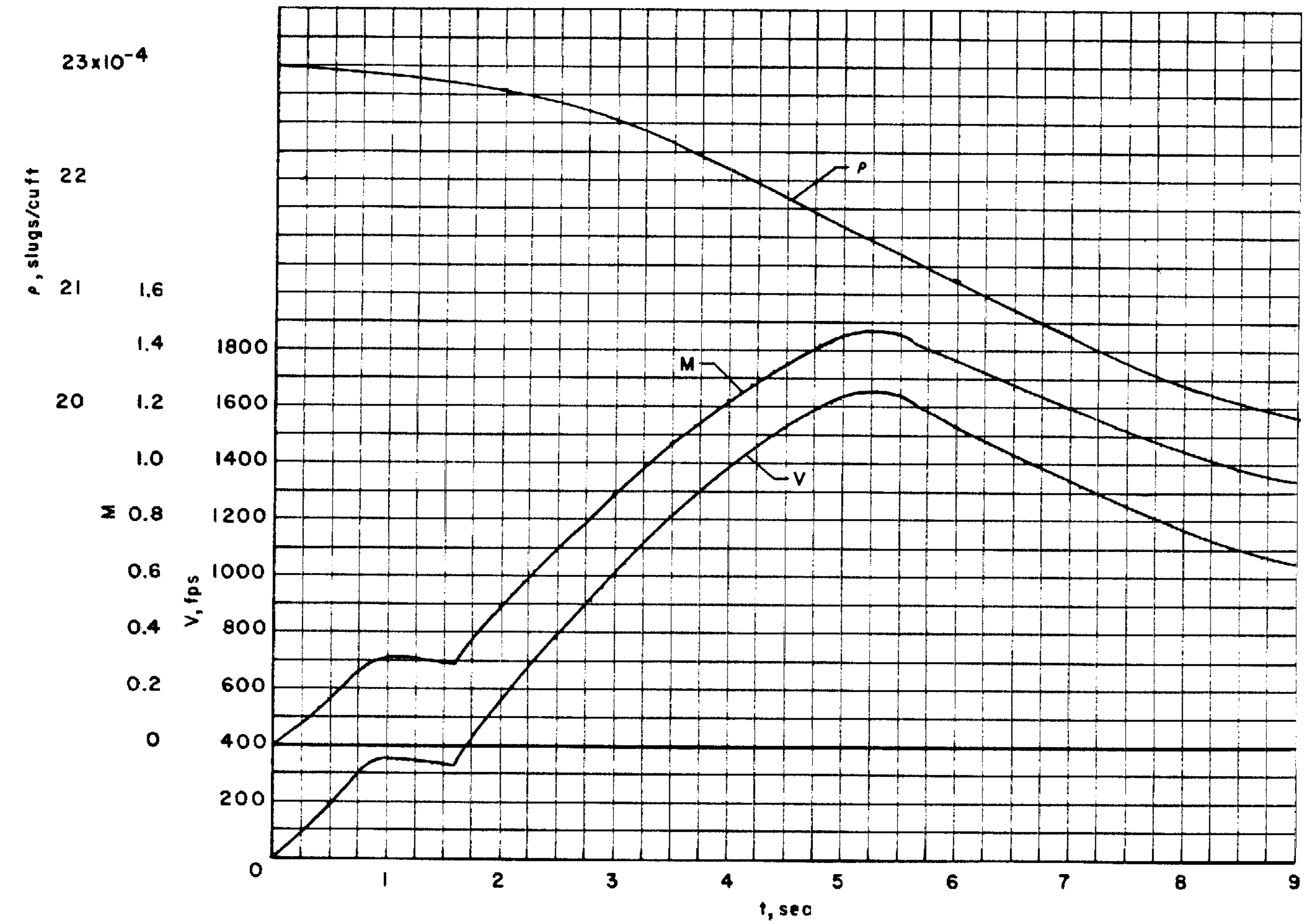

(c) Model 3.

Figure 5.- Concluded.

[redacted]

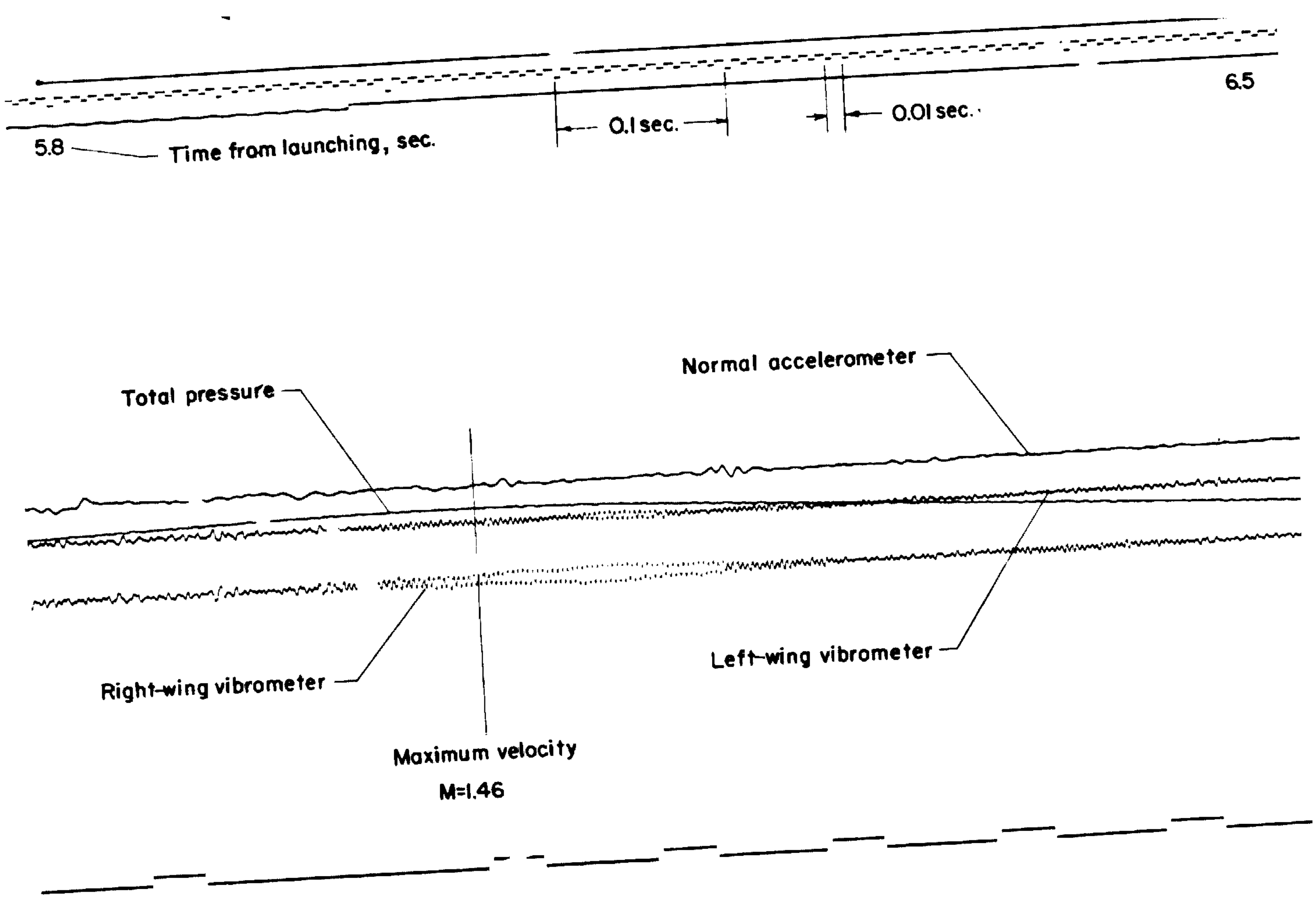

(a) Model 1.

Figure 6.- Portions of telemeter records.

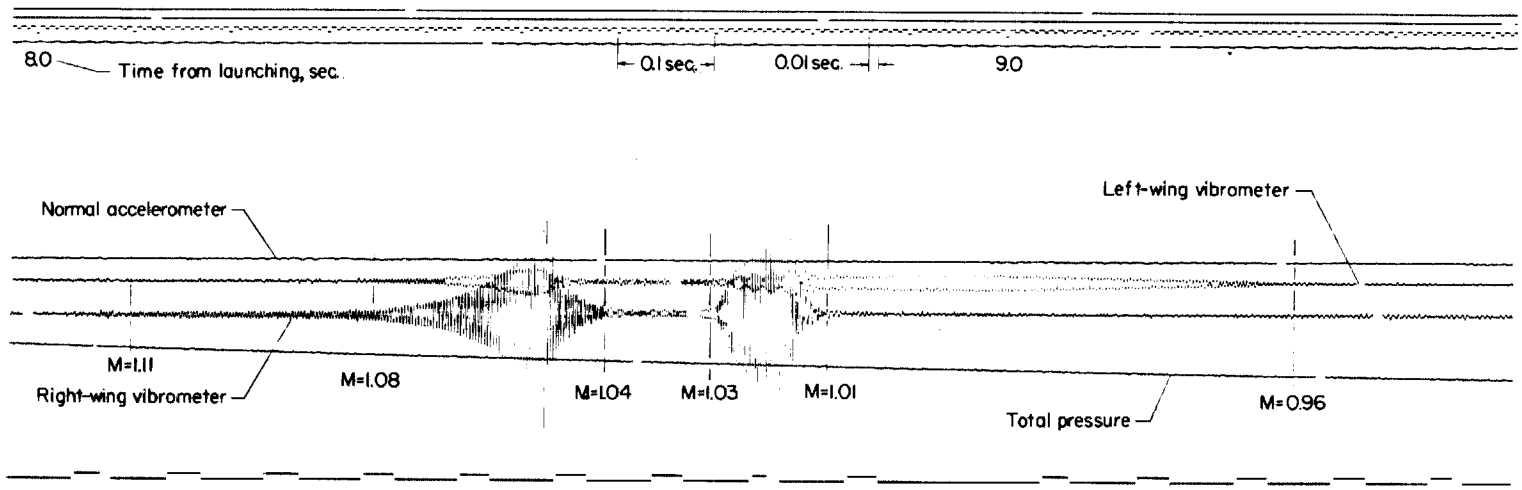

(b) Model 1, coasting.

Figure 6.- Continued.

[redacted]

[redacted]

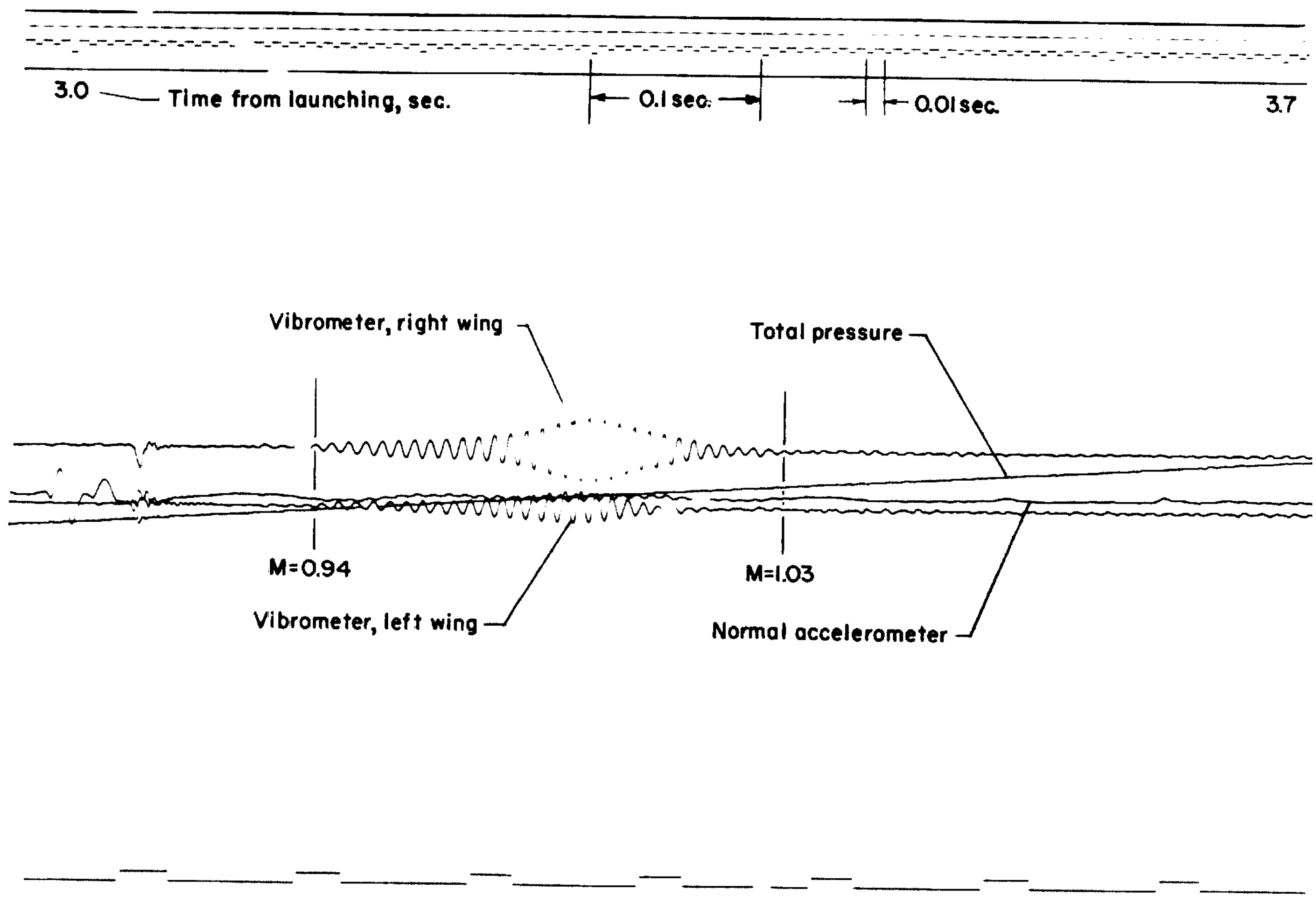

(c) Model 3.

Figure 6.- Concluded.

[redacted]

 [redacted]

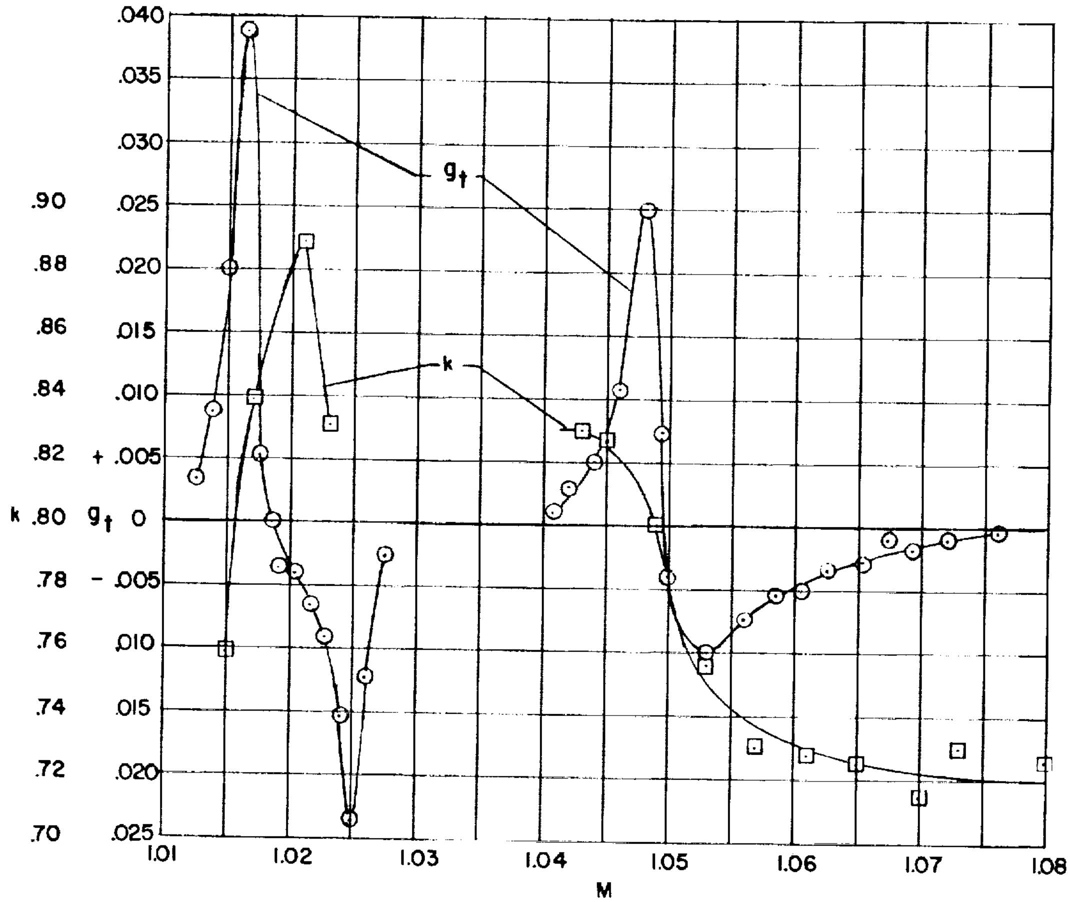

(a) Model 1.

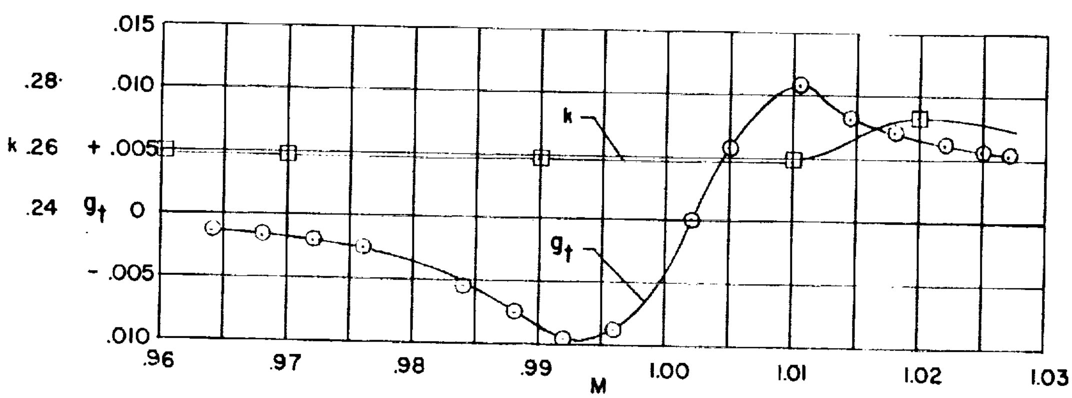

(b) Model 3.

Figure 7.- Variation of total damping coefficient with Mach number.

[redacted]

INDEX

Subject	Number
Wings, Complete	1.2.2
Airplanes - Specific Types	1.7.1.2
Vibration and Flutter - Wings and Ailerons	4.2.1

ABSTRACT

Results of flutter tests on three pairs of 1/10-scale Republic F-105 airplane wings in the subsonic to low supersonic speed range by use of rocket-propelled vehicles are presented. These wings had mass ratios nearly equal to the full-scale wings and were of less stiffness, one pair being weaker than the other two.

[redacted]